Biomed Microdevices (2007) 9:523–531
DOI 10.1007/s10544-007-9060-8

A microfabricated platform probing cytoskeleton dynamics using multidirectional topographical cues

Junyu Mai · Cheng Sun · Song Li · Xiang Zhang

Published online: 22 May 2007

Abstract Cell migration, which involves complicated coordination of cytoskeleton elements and regulatory molecules, plays a central role in a large variety of biological processes from development, immune response to tissue regeneration. However, conventional methods to study in vitro cell migration are often limited to stimulating a cell along a single direction or at a single location. This restriction prevents a deeper understanding of the fundamental mechanisms that control the spatio-temporal dynamics of cytoskeleton. Here we report a novel microfabricated platform that enables a multi-directional stimulation to a cell using topographical cues. In this device, cells were seeded on a grid-patterned topographically structured surface composed of 2 μm wide and 2 μm high straight ridges. Because the size of a unit grid was smaller than a single cell, each cell was simultaneously experiencing contact guidance leading to different directions. The device showed that healthy cells preferred to align and migrate in the direction of the longer side of the grid. But cells with impaired intracelluar tension force generation exhibited multiple uncoordinated cell protrusions along guiding ridges in all directions. Our results demonstrate the importance of actomyosin network in long-range communication and regulation of local actin polymerization activities. This platform will find wide applications in investigations of signal transduction and regulation process in cell migration.

Keywords Cell migration · Cytoskeleton · Surface topology · Microtexture · Smooth muscle cell · Cell-substrate interaction · Contact guidance · Single cell manipulation

J. Mai · C. Sun · X. Zhang (✉)
NSF Nanoscale Science and Engineering Center,
University of California, 5130 Etcheverry Hall,
Berkeley, CA 94720, USA
e-mail: xiang@berkeley.edu

J. Mai · S. Li
UCSF/UC Berkeley Joint Graduate Group in Bioengineering,
University of California, Berkeley, CA 94720, USA

1 Introduction

Cell migration plays a central role in wide varieties of biological processes involved in both normal physiology and in pathology. During the embryonic development, cell migration is critical for morphogenesis and neuron wiring. In adult organism, migration of leukocytes, fibroblasts and many other cells contributes to immune response and tissue regeneration. Abnormal cell migration are linked to diseases such as metastasis and atherosclerosis (Lauffenburger and Horwitz 1996; Ridley et al. 2003). Therefore it is important to understand how a cell can coordinate its molecular components to migrate toward its target correctly. Various factors, such as different chemoattractants, temperature, adhesiveness, rigidity and topography of the extracellular matrix (ECM), can stimulate different signal transduction pathways leading to cytoskeleton reorganization and affect cell migration. Additionally, attractions of the same type may stimulate different areas of the cell, for example, two bacteria running in two directions in front of a neutrophil (Rogers 1950). Therefore when living in a complex and dynamic *in vivo* environment filled with multiple attractions, a cell must respond in a controlled manner to orient and migrate toward the most important signal. This requires a comparison of the attractions that the

cell is encountering at different part of the membrane, and a global coordination of cytoskeleton elements. However, despite our increasing understanding of cell migration toward a single target, how a cell responds to multiple stimuli in a more realistic environment remains elusive.

A major hurdle in further study of the spatiotemporal dynamics of cell migration lies in the inability to quantitatively stimulate the cell membrane at multiple localized areas. Besides studying random cell migration on a homogeneous flat surface, methods to stimulate a directional cell migration include artificial wounding by scratching a cell monolayer, and creating a chemoattractant gradient by Boyden chamber (Ponath et al. 2000), Dunn chamber (Zicha et al. 1997), micropipettes, scattered beads, or microfluidics (Jeon et al. 2002). Despite their many attributes and capabilities, such methods only give us limited ability for cell manipulation, because stimulations affect a large area on the cell membrane and can hardly be applied from more than one direction. Also, in these systems, spatial distribution of environmental guidance cues, such as concentration of chemoattractants, cannot be easily visualized in the presence of the cell to allow correlation of extracellular stimulation with dynamic intracellular responses. There were attempts to simultaneously stimulate a cell with fluorescently labeled chemoattractant from two different directions (Janetopoulos et al. 2004), but the cells had to be completely immobilized to avoid perturbing of the gradient during the experiments. Tools such as atomic force microscopy (AFM), magnetic tweezers, and optical laser tweezers had been successfully applied to stimulate one local area on the cell membrane (Choquet et al. 1997; Bausch et al. 1999; Wang et al. 2005; Prass et al. 2006). Although theoretically stimulations on multiple locations are possible using these point-based methods, potential problems of cross-talking and interferences between manipulators, plus high cost of system setup, may limit their wide application in general laboratories for life science research.

Contact guidance describes the phenomenon that fibroblast-like cells and axons of neurons preferentially align and migrate along straight ridges and grooves (Weiss 1945). It is found that stress fibers and focal adhesions of the cells preferentially align along the guiding ridges. Using current fabrication technology, topographical structured substrate at micrometer or even nanometer scale resolution had been prepared for cell culture and to study cell response (Clark et al. 1991; Flemming et al. 1999; Desai et al. 1999; Frey et al. 2006; Teixeira et al. 2006). Molecular mechanism of a cell's sense of substrate geometry is being explored to understand how topographical features are recognized by the cell and how they regulate cell behavior (Vogel and Sheetz 2006). Compared to other cell manipulation methods, topographical guidance are stable, visible, spatially confined and can be arbitrarily patterned. However, since previous studies on contact guidance are mostly on parallel straight lines, the potential of using topographical feature as a cell manipulation tool has not been fully explored yet.

In this paper, we demonstrate that we can use a microfabricated device with a grid patterned topographically structured surface (TopoSurface) to apply stimulations in the form of contact guidance to a single cell from multiple directions (Fig. 1). Because different local parts of the cell will protrude toward different directions in response to the guiding ridges that the cell membrane is in touch with, the cell is constantly experiencing multi-directional guidance. We ask how these remote local reactions at different parts

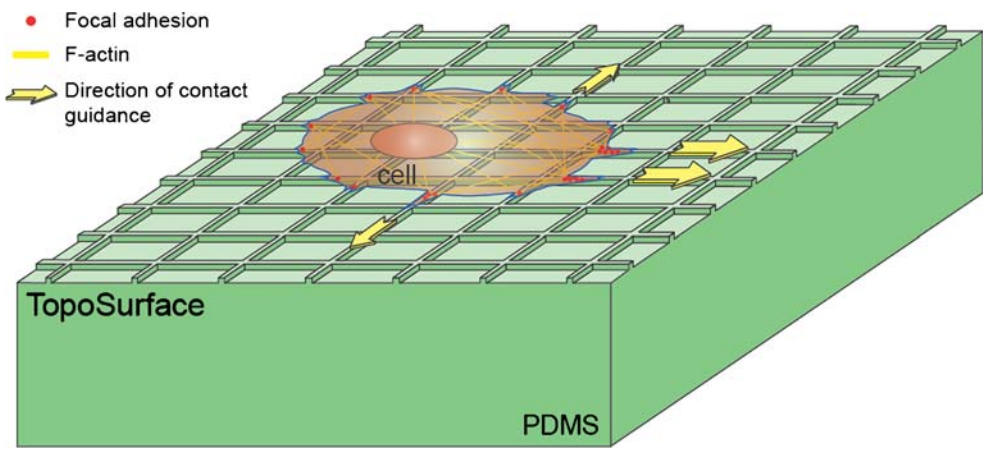

Fig. 1 Schematic of applying multi-directional contact guidance to a cell using grid patterned TopoSurface. The figure illustrates a cell migrating from left to right on a PDMS substrate molded with grid patterned topographical texture. In response to the guiding ridges under the cell membrane, the cell is protruding toward different directions, led by focal adhesions and actin filaments along the guiding ridges. We ask how remote local activities of actin polymerization communicate with each other, and how a cell globally regulates these local reactions to maintain its migration direction

of a cell communicate with each other, and how a cell globally regulates these local activities. We use bovine aortic smooth muscle cells (BASM) to demonstrate that migrating cells have the ability to compare the guidance from different directions and selectively follow the dominant guidance, which is along the longer side of a rectangular grid. Furthermore, disruption of the intracellular tension force by Blebbistatin or Y27632 results in multiple membrane protrusions led by guiding ridges in all directions.

2 Materials and methods

2.1 Fabrication of TopoSurfaces

We fabricated TopoSurfaces using standard softlithography techniques (Whitesides et al. 2001). We used computer aided design software L-edit and AutoCAD to design the 2D patterns. A Chromium mask was generated from the designed pattern (UC Berkeley Microlab) at a 1:1 reduction ratio and used for photolithography. A 4-inch silicon wafer was treated with Hexamethyl Disilazane (HMDS) for 5 min to improve photoresist adhesiveness and spin coated with photoresist S1818 (Shipley) at 15,000 rpm for 30 s. S1818 was soft baked on a 90°C hot plate for 2.5 min before photolithography. The patterns were transformed from the chromium mask to S1818 by contact lithography (Qintel) at an exposure strength of 5.8 mW/cm^2 for 20 s. After pattern exposure, non-crosslinked S1818 was gently removed in MicroDev (Rohm and Haas) (1:1(v/v) dilution in deionized water). The resulting photoresist mold was examined under microscope and then hard-baked in a 120°C oven (VWR) for 30 min. Poly(dimethylsiloxane) (PDMS) and its curing agent (Sylgard 184, Dow Corning) were thoroughly mixed at 10:1 (w/w) ratio and poured onto the photoresist mold in a 100 mm petri dish container (Corning). The container was left at room temperature on a flat surface for 48 h. After PDMS was cured, it was cut and peeled off from the wafer, and subsequently rinsed in acetone, deionized water and 2-proponal to be cleaned and sterilized. Before cell culture, the PDMS substrate was coated with 20 μg/ml fibronectin (Sigma Aldrich) for 30 min at room temperature and rinsed with phosphate buffered saline (PBS).

2.2 Cell culture and imaging

Primary bovine aortic smooth muscle cells (BASM) between passages 2 and 14 were used for experiments. BASM were maintained in D-MEM (Invitrogen) plus 10% Fetal Bovine Serum (Hyclone) at 37°C and 5% CO_2 in 10 mm tissue culture dishes (Corning). Before experimentation, confluent cells were detached from the dish by 0.05% trypsin-EDTA(Invitrogen), and seeded onto the fibronectin coated PDMS substrate at 1:5–1:10 dilution ratio. 50 uM of (-)-Blebbistatin(Sigma Aldrich), 20 uM of Y27632 (InSolution, Calbiochem), or 20 uM of ML-7 (Calbiochem) was added to the cell culture at the time of plating or after 24 h, depending on the experiment. Cells were incubated at 37°C and 5% CO_2. For F-actin staining, cells were fixed with 4% fresh formaldehyde (Sigma Aldrich) for 20 min, and permeablized with 0.1% Triton-X 100 (Sigma Aldrich) for 5 min. Cells were stained with Rhodamine-Phalloidin (Invitrogen) for 20 min and DAPI (Invitrogen) for 5 min. PBS rinsing was performed between incubations. For vinculin staining, cells were fixed with

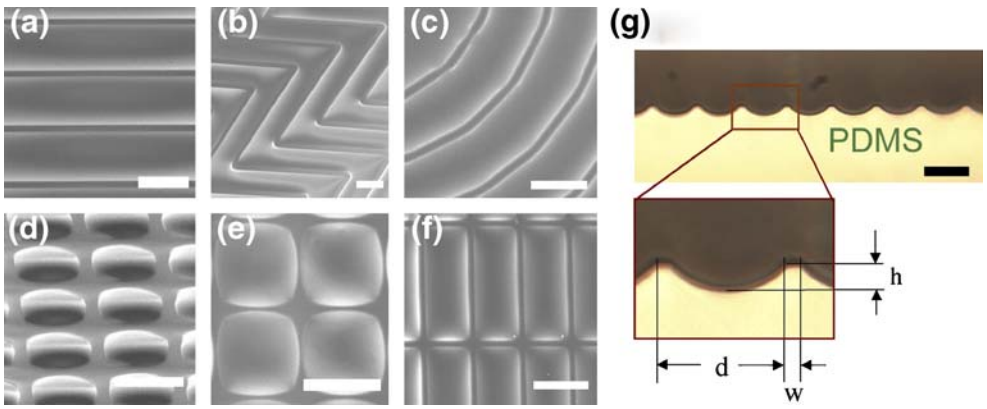

Fig. 2 Topology of TopoSurfaces. (**a**–**f**) Scanning electronic microscope (SEM) images of PDMS substrates with different patterns: (**a**) 20 μm spaced parallel straight ridges; (**b**) 20 μm spaced zigzagging ridges with 60° turning angle; (**c**) 20 μm spaced concentric circular ridges; (**d**) 9 μm×20 μm grid; (**e**) 20 μm×20 μm grid; and (**f**) 20 μm×50 μm grid. (**g**) optical image of the cross section of a TopoSurface with 20 μm spaced ridges. *Scale bar*, 20 μm. *h* is the height of the ridges, 4±10% μm, and varies from 2 to 4 μm in different patterns. *d* is the distance between two adjacent ridges, 20±1% μm. *w* is the width of a ridge, 2.1±10% μm. Note that the top of the ridges were sharp, providing contact guidance to the cells; but the bottom of the ridges were smoothly curved, avoiding blocking of cell migration with deep corners at the bottom

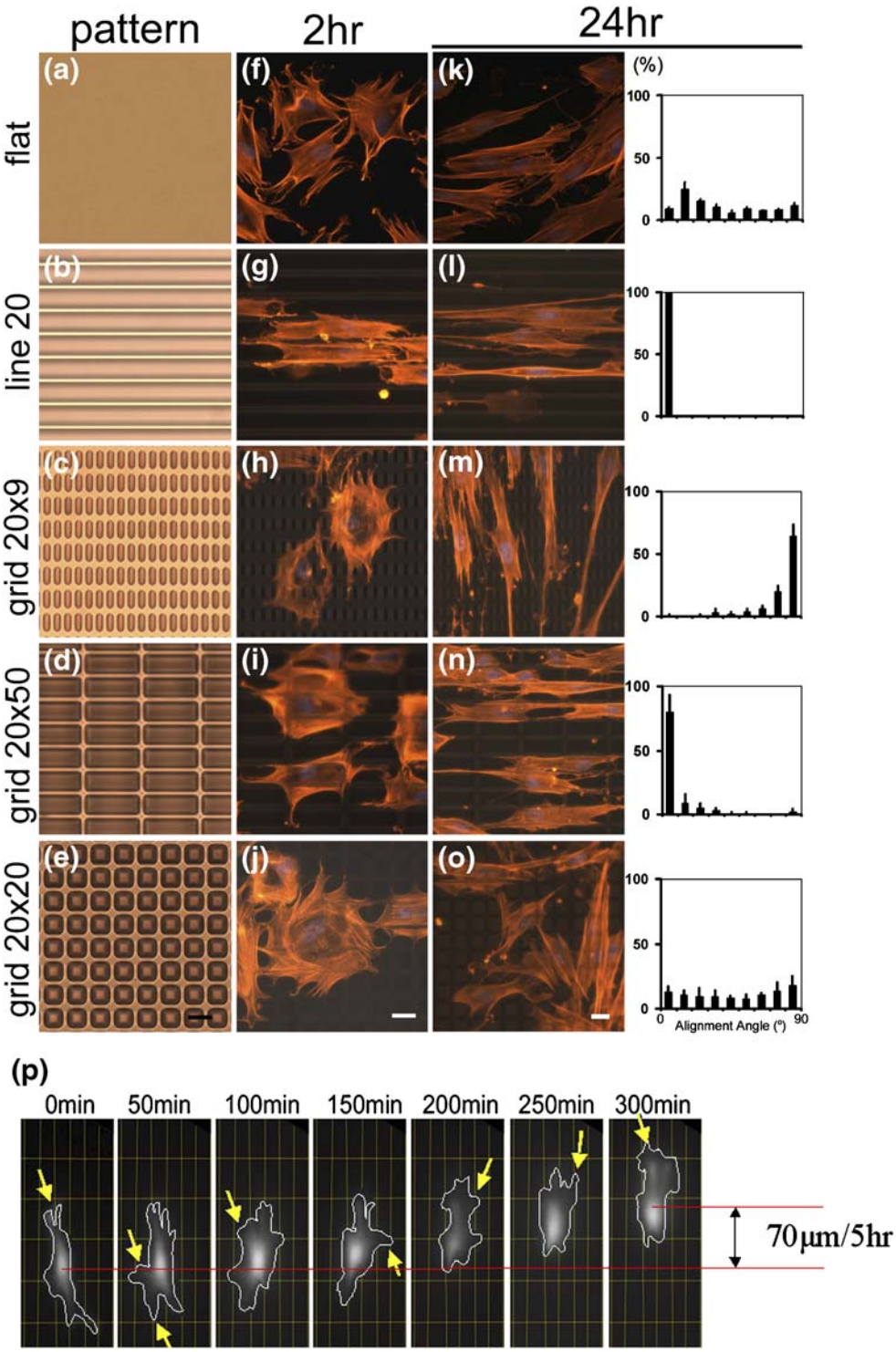

Fig. 3 Alignment and migration of BASM under multi-directional topographical guidance. (**a**–**e**) optical images of TopoSurfaces. (**f**–**j**) F-actin of BASMs being cultured for 2 h on the TopoSurface, revealing protrusions along guiding ridges in all directions. (**k**–**o**) F-Actin of BASMs (*left*) and histogram of cell alignment angles (*right*) after 24 h culture on the TopoSurface. *Error bars* are the averaged deviations. *Scale bars*, 20 μm. (red: Rhodamin-Phalloidin, blue: DAPI) (**p**) Time-lapse fluorescent microscope images of a GFP-transfected BASM migrating on a 20×50 grid pattern. Substrate pattern were highlighted in yellow. *Arrows* point to protrusions extended along guiding ridges

−20°C acetone and stained with anti-Vinculin FITC conjugated antibody (Invitrogen) for 2 h. The sample was mounted onto glass coverslip with Slowfade mounting media (Invitrogen) and sealed with nail polisher. The sample was imaged under Zeiss Axiophot epifluorescent microscope with Photometrics Quantix cooled digital CCD camera and Qimaging MicroPublisher software.

2.3 Timelapse fluorescent microscopy

Cells were transfected with GFP plasmid using Lipofectamine 2000 (Invitrogen) and manufacturer suggested protocol. For timelapse image aquisition, transfected cells were cultured on a TopoSurface and maintained at 37°C in CO_2 Independent Media (Invitrogen) on fluorescent

microscope stage (Nikon). Fluorescent images were taken every 10 min for 5–10 h using Metamorph Imaging System (Molecular Devices).

2.4 Measurement of cell alignment angles

On grid and line patterns, alignment angles were the angle between the axis of cell body and the 20 μm spaced ridges. On flat surface, the angle was measured against a randomly picked straight line. All angles were symmetrically folded to 0–90° range. Data were generated from three independent experiments. 30–90 randomly picked cells were analyzed for each pattern in each experiment. In Fig. 3(k–o), the *Y* axis is the percentage of cells within a certain range of alignment angle over the total number of cells on the same patterned surface. Error bars are the averaged deviations.

3 Results

3.1 Distinct cell alignment pattern under multi-directional guidance on TopoSurfaces

We designed and fabricated grid patterns with different distances between neighboring guiding ridges: 20 μm by 50 μm (20×50), 20 μm by 9 μm (20×9), 20 μm by 20 μm (20×20), and straight parallel ridges 20 μm apart (line 20) as control (Fig. 2). The ridges were about 2 μm wide and 2–4 μm high, depending on the density of the ridges. The unit grid size of these patterns was designed to be smaller than a single BASM, which averages 30 μm wide and 80 μm long, so that each cell on the grid would be constantly exposed to multi-directional stimulations while migrating. The 20×20 pattern would present equal guidance to a cell in two orthogonal directions, while the 9×20 and 20×50 patterns have different density of guiding ridges along two orthogonal directions.

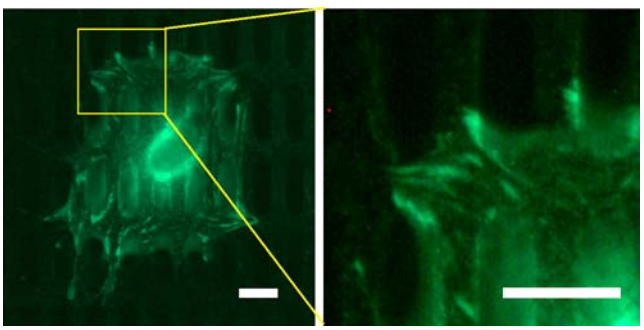

Fig. 4 Focal adhesions on grid patterened TopoSurface. A representative BASM stained with FITC-conjugated anti-Vinculin antibody after culturing on 20×9 grid patterned TopoSurface for 2 h, showing focal adhesions along guiding ridges. *Scale bars*, 10 μm

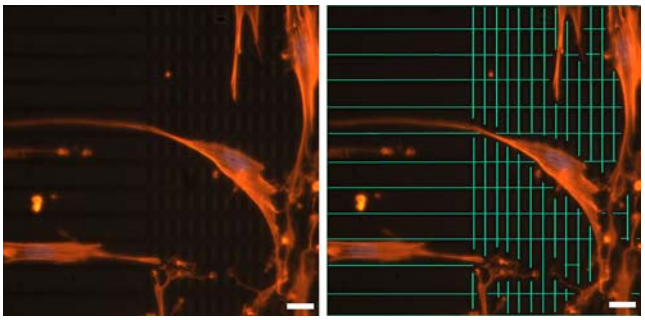

Fig. 5 Reorganization of cytoskeleton on different substrate patterns. A cell changing its orientation when moving from a line20 pattern to a 20×9 grid pattern, with its tail at the line20 pattern and the front at the 20×9 pattern. This demonstrates the cell's accurate sensing of the substrate topographical pattern and coordination of cytoskeleton toward the strongest guidance. *Left*: Original image showing substrate pattern in the background. *Right*: Substrate pattern highlighted in green for easy visualization. *Scale bar*, 20 μm. (red: Rhodamin-Phalloidin, blue: DAPI)

Interestingly, BASM responded to the grid in a highly sensitive yet coordinated manner. Within 2 h after plating on the pattern substrate, cells began to extend protrusions along the guiding ridges in all directions around the cell body (Fig. 3(f–j)). Focal adhesions were mostly clustered along the ridges (Fig. 4). After 24 h, cells elongated on all patterns and aligned in distinct, pattern-dependent fashions (Fig. 3(k–o)). On the 20×20 grids, cell alignment was random (Fig. 3(o)), similar to that on a flat surface (Fig. 3(k)). On rectangular grids, cells elongated and migrated specifically in the direction of the longer side of the grid (Fig. 3(m,n)). Time-lapse recording of Green Fluorescent Protein (GFP)-transfected BASM (Fig. 3(p)) showed that during migration, cells protruded along the ridges both at the front and on the side of the cell body. However extensions along side ridges were retracted in about 100 min, whereas protrusions along the direction of denser and longer ridges were strengthened, resulting in a persistent polarity and migration direction. When traveling across the border of two patterns, cells could change their migration direction accordingly (Fig. 5), demonstrating an accurate response to the underlying patterns.

3.2 High degree of cytoskeleton flexibility exhibited on zigzagging patterned TopoSurface

To understand whether the rigidity of the cytoskeleton maintains a cell's elongated shape and prevents it from extending along crossing guiding ridges on the grid patterned TopoSurface, we plated cells on zigzagging patterned TopoSurfaces with different turning angles. We found that within 2 h, the cells flexibly reorganized their actin cytoskeletons to follow the zigzagging guiding ridges (Fig. 6(a)). Depending on the length of each individual cell, a single

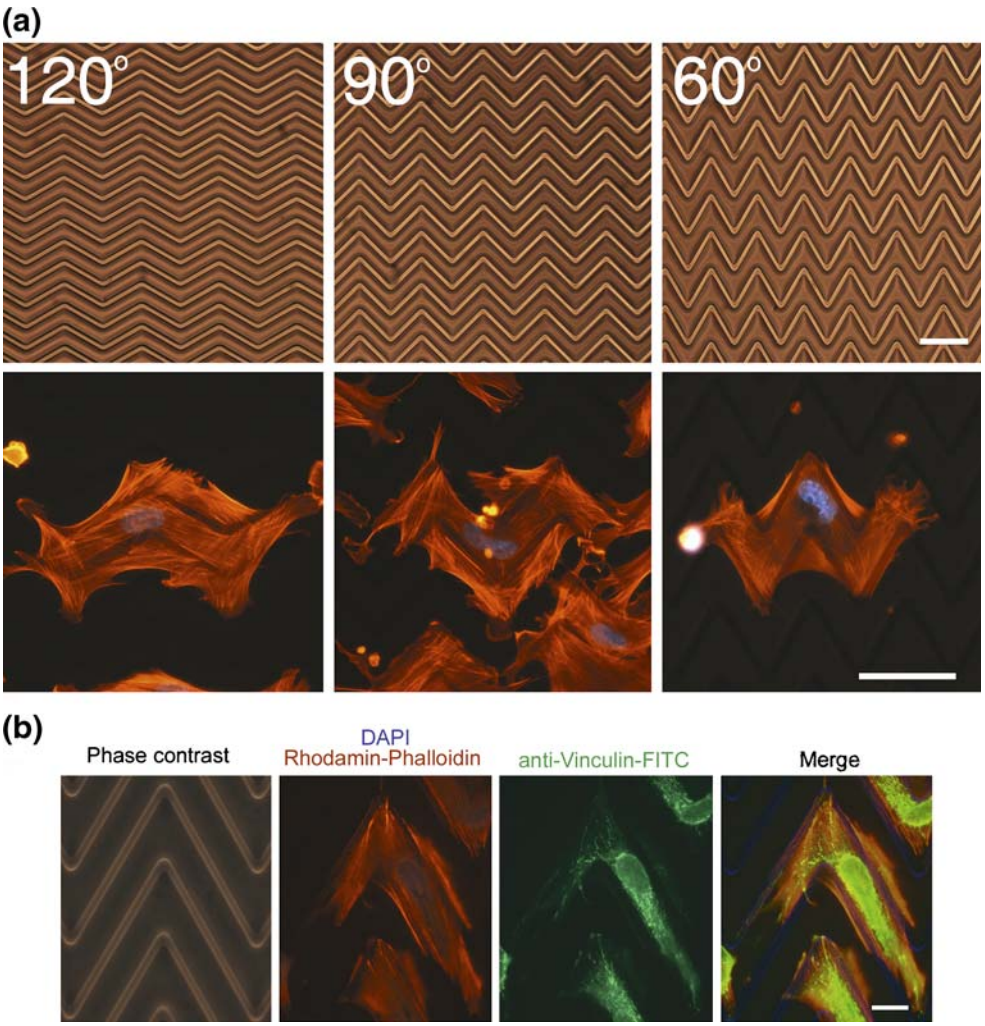

Fig. 6 Reorganization of actin cytoskeleton on a zigzagging patterned TopoSurface, demonstrating that the rigidity of the cytoskeleton does not prevent a normally elongated cell from making sharp turns when the cell is properly guided. (**a**) BASM were plated on zigzagging patterned TopoSurfaces with bending angles of 120, 90 or 60° for 2 h at sub-confluent density to avoid cell-cell contact. Cells were then fixed and stained. *Upper panels:* optical image of the patterns on the substrate; *Lower panels:* single cell actin cytoskeleton on corresponding TopoSurfaces (red: Rhodamin-Phalloidin, blue: DAPI). (**b**) A representative fluorescent image of a BASM cultured on a 60° zigzagging TopoSurface, showing the actin cytoskeleton and focal adhesions. In the merged image, color of the guiding ridges is changed to blue for easy visualization

cell body could be guided to turn 1–3 times. Stress fibers were kept straight and anchored by focal adhesions when a cell was turning (Fig. 6(b)). Therefore, the rigidity of the cytoskeleton is not the limiting factor in preventing a cell from following guiding ridges in changing directions.

From the above results, we interpret the consistent alignment pattern of cells on rectangular grid pattern as the result of the cells' active and selective response to the strongest contact guidance among all the guidance from multiple directions. Along the longer side of the grid, both the density and length of the guiding ridges are larger than that along the shorter side of the grid. Thus the guiding effect along the longer side of the grid is stronger. Actin polymerization in response to minor attractions was not inhibited from the beginning; rather, it was initiated first and then quickly suppressed even though the guidance remained the same. The behavior of the cell facing multiple guidance revealed a global comparison and regulation system, allowing the cell to selectively inhibit actin polymerization toward minor directions.

3.3 Inhibition of myosin II contractility caused un-coordinated multi-directional protrusions on grid patterned TopoSurfaces

To investigate whether force generation and transmission inside the cell is involved in the regulation of local actin polymerization activities, we treated cells with 50 μM Blebbistatin, a specific inhibitor of myosin II contractility (Straight et al. 2003), and seeded the cells on grid-patterned TopoSurface. Two hours after plating, all cells extended multiple protrusions along the guiding ridges (Fig. 7), showing unaffected abilities of topography sensing, actin polymerization and membrane protrusion. However, unlike the protrusions of the untreated cells, which were short, stress fiber rich, and interconnected with the central actomyosin network (Fig. 7(a–e)), protrusions of cells treated with Blebbistatin were long and contained no stress fibers (Fig. 7(f–j)). They freely turned or branched when reaching a crossing ridge. And the main cell bodies did not have consistent, grid pattern dependent orientations as the

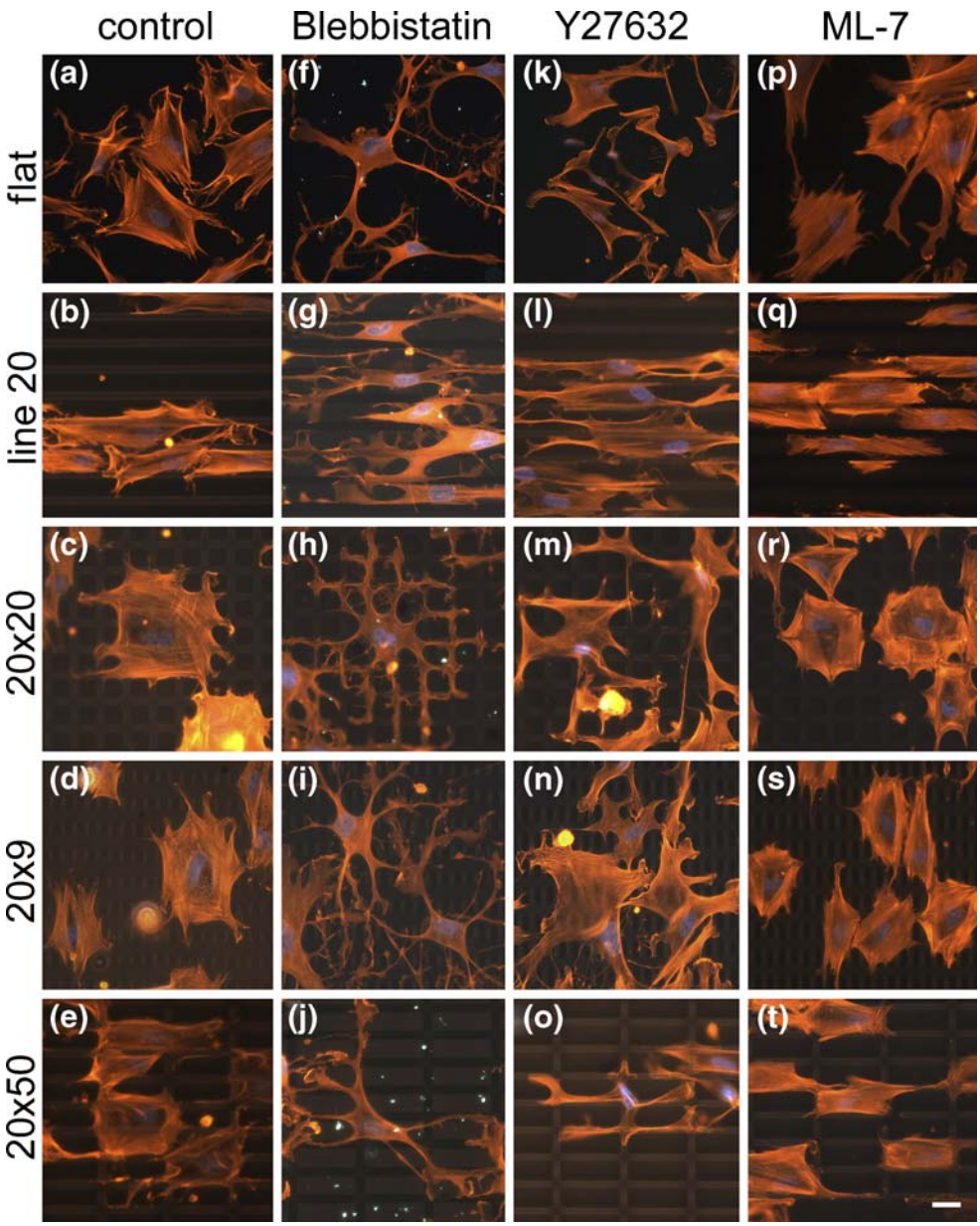

Fig. 7 Coordination of actin cytoskeleton on grid surface during cell spreading is inhibited by Blebbistatin and Y27632, but not ML-7. (**a**–**e**) F-acitn of untreated cells cultured on different patterns for 26 h. (**f**–**t**) F-actin of inhibitor treated cells spreading on patterned substrates. Inhibitors were added to cell suspension during plating and cells were fixed and stained after 2 h incubation. *Scale bar*, 20 μm. (red: Rhodamin-Phalloidin, blue: DAPI)

untreated cells did. The only exception is on the line20 pattern (Fig. 7(g)), where guiding ridges were in parallel directions and Blebbistatin treated cells still elongated along the ridges. These results indicate the requirement of myosin II contractility in global regulation of local actin polymerizations.

Rho Kinase (ROCK), Myosin Light Chain Kinase (MLCK), and Zipper Interaction Protein (ZIP) kinase were shown to have the capability of phosphorylating myosin II in smooth muscle cells (Kureishi et al. 1997; Ikebe and Hartshorne 1985; Komatsu and Ikebe 2004). To test the involvement of these possible upper stream regulators, we mixed cells with 20 μM Y27632, a specific ROCK inhibitor, and 20 μM ML-7, an inhibitor to both MLCK and ZIP kinase (Komatsu and Ikebe 2004), before plating the cells on grid-patterned substrates. Cells treated with ML-7 showed no impairment in establishing correct orientations on the grid (Fig. 7(p–t)), although they displayed characteristically less spreading cell shape and decreased peripheral stress fibers (Katoh et al. 2001). On the contrary, cells treated with Y27632 behaved very similarly as those treated with Blebbistatin (Fig. 7(k–o)).

We also added inhibitors to cells that had been cultured on the grid patterns for 24 h and with established polarity (Fig. 8). Before adding inhibitors, all cells had an elongated cell shape. Three hours after being treated with Blebbistatin or Y27632, some cells maintained their polarity with an elongated cell body and tapered tail, but had a broad and

grid-guided multi-directionally branched front (Fig. 8(h,i,o); others had long protrusions all over the cell body (Fig. 8(m,n,j)). The reason of the two different phenotypes remains unclear. It is possibly related to the distribution of intracellular active molecules when the inhibitors were added. Again, there was no noticeable difference between ML-7 treated and untreated polarized cells. The results indicate that myosin II and ROCK, but not MLCK or ZIP kinase, are required for coordinated actin polymerization, before and after the cell has established its polarity. This also suggests that the coordination is possibly mediated through the Rho-Rock-Myosin II signal transduction pathway (Kimura et al. 1996; Jaffe and Hall 2005).

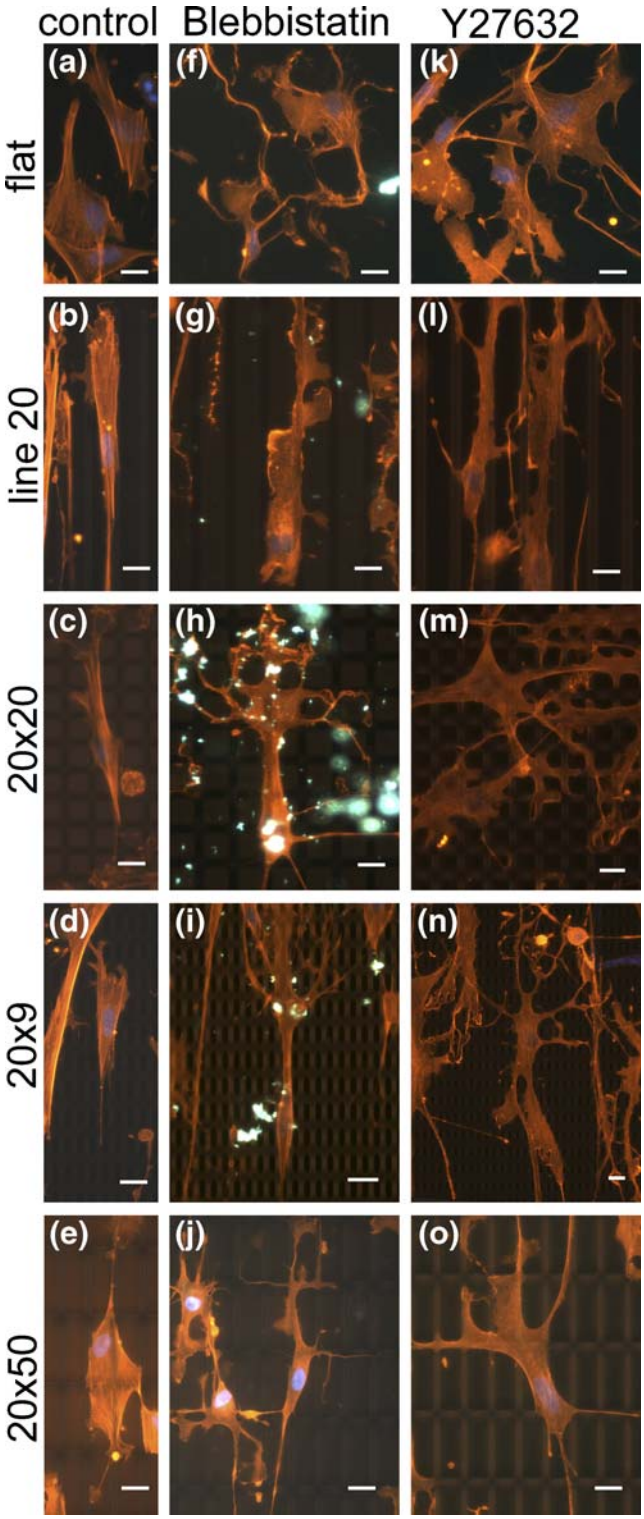

Fig. 8 Effect of Blebbistatin and Y27632 on polarized cells on TopoSurfaces. (**a**–**e**) Control cells cultured for 27 h without inhibitor. (**f**–**o**) After culturing for 24 h, BASMs were treated with inhibitors for 3 h. *Scale bars*, 20 μm. (red: Rhodamin-Phalloidin, blue: DAPI)

4 Discussion

It is well known that traction force generated by actomyosin network is required for a cell to migrate forward (Lauffenburger and Horwitz 1996). Besides this basic function, more and more evidence indicate that the myosin II mediated contraction plays a central role in coordinating adhesion, protrusion and actin organization (Schwartz and Horwitz 2006). Recent studies demonstrated that myosin II generated tension affects the rate of adhesion assembly and disassembly (Gupton and Waterman-Storer 2006), and is involved in propagation of active Src molecules (Wang et al. 2005). In addition, increased tension has an inhibitory effect on Rho Family GTPase Rac (Katsumi et al. 2002), which regulates actin polymerization (Jaffe and Hall 2005). But for a cell to sense its direction in a chemoattractant gradient, actomyosin network does not seem to be required (Parent and Devreotes 1999; Janetopoulos et al. 2004), because inhibition of myosin II or ROCK did not prevent the cells from constructing protrusions toward the correct direction (Xu et al. 2003; Kolega 2003). However these observations and conclusions were obtained from experiments with cells migrating toward a single stimulation source. We demonstrate that when facing attractions from multiple directions, without actomyosin contractility, a cell cannot down-regulate actin polymerization in minor directions. Since different external stimulations can eventually be transduced into mechanical force through myosin II activation, it is possible that by the contraction of the actomyosin network throughout the cell, stimulations at different locations and of different origins, chemical, topographical and other, are compared. And the result of comparison, in the form of mechanical signal, is converted back to chemical signals to regulate local actin polymerizations.

For the study of cytoskeleton dynamics under multi-directional stimulations, a grid patterned TopoSurface offers several advantages over conventional gradient-based stimulation methods: (1) Guidance cues can be confined at a small local area (less than 2 μm) on the cell membrane, so that stimulations applied from different directions will not

overlap; (2) Guidance cues are visible in the presence of the cell, allowing clear mapping between the extracellular stimulation and intracellular response; (3) Guidance remain stable during cell migration, which enables long term observation and helps us to interpret the dynamical intracellular reactions by minimizing external variations; (4) TopoSurface does not block cell adhesion or migration as contact printing method (Mrksich et al. 1996); and (5) A substrate with TopoSurface could be easily replicated and conveniently handled for cell culture, staining and imaging.

For future studies, more details of the regulation mechanism could be revealed by combining this device and other advanced optical imaging methods. For example, we can use fluorescence resonance energy transfer (FRET) based protein activity sensor (Kraynov et al. 2000; Wang et al. 2005; Pertz et al. 2006) to directly monitor the aggregation or activation of key regulating molecules when the cell is interacting with the short and long ridges on the grid patterned TopoSurface.

5 Conclusions

We designed and fabricated a platform with microstructured topographical surface pattern to study spatial-temporal dynamics of cytoskeleton. Using this device, we can bend a single cell cytoskeleton to from 120, 90 and even 60° angles using zigzagging patterns, and we can automatically provide multi-directional contact guidance to a single migrating cell using sub-cellular scale grid patterns. We found that despite high degree of flexibility and sensitivity, cells have the ability to compare migration guidance from different directions and selectively follow the dominant guidance. However, disruption of the intracellular tension force resulted in multiple uncoordinated membrane protrusions led by guiding ridges in all directions. Our results demonstrate the importance of actomyosin network in regulating actin polymerization activities, and the usefulness of the TopoSurface platform in studying dynamic molecular and cellular response during cell migration.

Acknowledgements We thank A. Fisher at Berkeley Tissue Culture Center, S. Ruzin and D. Schichness at Berkeley Biological Imaging Facility, D. Drubin's lab, and J. Chu for help in cell culture and imaging. We thank JS. Xu and S. Wang for comments on the manuscript. This work was supported by the Center for Cell Mimetic Space Exploration and NSF Nanoscale Science and Engineering Center. J. M. is supported by NSF-IGERT fellowship.

References

A.R. Bausch, W. Moller, E. Sackmann, Biophys. J. **76**(1), 573 (1999)
D. Choquet, D.P. Felsenfeld, M.P. Sheetz, Cell **88**(1), 39 (1997)
P. Clark, P. Connolly, A.S.G. Curtis, et al., J. Cell Sci. **99**, 73 (1991)
T.A. Desai, D. Hansford, M. Ferrari, J. Membr. Sci. **159**(1–2), 221 (1999)
R.G. Flemming, C.J. Murphy, G.A. Abrams, et al., Biomaterials **20**(6), 573 (1999)
M.T. Frey, I.Y. Tsai, T.P. Russell, et al., Biophys. J. **90**(10), 3774 (2006)
S.L. Gupton, C.M. Waterman-Storer, Cell **125**(7), 1361 (2006)
M. Ikebe, D.J. Hartshorne, J. Biol. Chem. **260**(18), 27 (1985)
A.B. Jaffe, A. Hall, Rho GTPase: biochemistry and biology. Annu. Rev. Cell Dev. Biol. **21**, 247–269 (2005)
C. Janetopoulos, L. Ma, P.N. Devreotes, et al., Proc. Natl. Acad. Sci. USA **101**(24), 8951 (2004)
N.L. Jeon, H. Baskaran, S.K.W. Dertinger, et al., Nat. Biotechnol. **20**(8), 826 (2002)
K. Katoh, Y. Kano, M. Amano, et al., J. Cell Biol. **153**(3), 569 (2001)
A. Katsumi, J. Milanini, W.B. Kiosses, et al., J. Cell Biol. **158**(1), 153 (2002)
K. Kimura, M. Ito, M. Amano, et al., Science **273**(5272), 245 (1996)
J. Kolega, Mol. Biol. Cell **14**(12), 4745 (2003)
S. Komatsu, M. Ikebe, J. Cell Biol. **165**(2), 243 (2004)
V.S. Kraynov, C. Chamberlain, G.M. Bokoch, et al., Science **290** (5490), 333 (2000)
Y. Kureishi, S. Kobayashi, M. Amano, et al., J. Biol. Chem. **272**(19), 12257 (1997)
D.A. Lauffenburger, A.F. Horwitz, Cell **84**(3), 359 (1996)
M. Mrksich, C.S. Chen, Y.N. Xia, et al., Proc. Natl. Acad. Sci. USA **93**(20), 10775 (1996)
C.A. Parent, P.N. Devreotes, Science **284**(5415), 765 (1999)
O. Pertz, L. Hodgson, R.L. Klemke, et al., Nature **440**(7087), 1069 (2006)
P.D. Ponath, J. Wang, H. Heath, Methods Mol. Biol. **138**, 113–120 (2000)
M. Prass, K. Jacobson, A. Mogilner, et al., J. Cell Biol. **174**(6), 767 (2006)
A.J. Ridley, M.A. Schwartz, K. Burridge, et al., Science **302**(5651), 1704 (2003)
D. Rogers, *Crawling Neutrophil Chasing a Bacterium*, http://www.biochemweb.org/fenteany/research/cell_migration/neutrophil.html (1950s)
M.A. Schwartz, A.R. Horwitz, Cell **125**(7), 1223 (2006)
A.F. Straight, A. Cheung, J. Limouze, et al., Science **299**(5613), 1743 (2003)
A.I. Teixeira, G.A. McKie, J.D. Foley, et al., Biomaterials **27**(21), 3945 (2006)
V. Vogel, M. Sheetz, Nat. Rev. Mol. Cell Biol. **7**(4), 265 (2006)
Y.X. Wang, E.L. Botvinick, Y.H. Zhao, et al., Nature **434**(7036), 1040 (2005)
P. Weiss, J. Exp. Zool. **100**(3), 353 (1945)
G.M. Whitesides, E. Ostuni, S. Takayama, et al., Annu. Rev. Biomed. Eng. **3**, 335 (2001)
J.S. Xu, F. Wang, A. Van Keymeulen, et al., Cell **114**(2), 201 (2003)
D. Zicha, G. Dunn, G. Jones, Methods Mol. Biol. **75**, 449–457 (1997)